

## Selection and reconstruction of the top quarks in the all-hadronic decays at a Linear Collider

S. V. Chekanov <sup>a</sup> and V. L. Morgunov <sup>b</sup>

<sup>a</sup> HEP Division, Argonne National Laboratory, 9700 S.Cass Avenue, Argonne, IL 60439 USA

<sup>b</sup> DESY, Notkestrasse 85, D-22603 Hamburg, Germany and ITEP, B.Chermushkinskaya, 25, Moscow, 117218, Russia

### Abstract

A method of reconstruction of the top quarks produced in the process  $e^+e^- \rightarrow t\bar{t} \rightarrow 6 jets$  at a Linear Collider (LC) is proposed. The approach does not involve a kinematic fit, as well as assumptions on the invariant masses of the dijets originating from the decays of  $W$  bosons and, therefore, the method is expected to be less sensitive to theoretical and experimental uncertainties on the top-mass measurement than traditional reconstruction methods. For the first time, the reconstruction of the top quarks was investigated using the full LC detector simulation after taking into account the background arising from QCD multi-jet production.

## 1 Introduction

The standard procedure of the top-quark measurements in the process  $e^+e^- \rightarrow t\bar{t} \rightarrow b\bar{b}q_1\bar{q}_2q_3\bar{q}_4 \rightarrow 6 jets$  takes advantage of a fully reconstructed final state. The decay signature is characterized by the production of six hadronic jets, therefore, a background arising from the standard six-jet QCD processes is expected. Nevertheless, since the all-hadronic top decay has the largest branching ratio ( $\simeq 44\%$  of all  $t\bar{t}$  decays), it is considered as one of the most promising at the TEVATRON, LHC and a Linear Collider (LC).

A reduction of the background from QCD multi-jet events can be achieved by identification of  $b$ -initialized jets (the so-called  $b$ -tagging). Furthermore, one can use the requirement that the invariant mass of two jets (not associated with the  $b$  quarks) is consistent with the decay of the  $W$  bosons. These two methods were used for the top reconstructions at the TEVATRON (see, for example, [1]), and also are considered for the LHC [2] and LC experiments [3, 4, 5].

The reconstruction of the top quarks in the all-hadronic decays is known to be affected by many theoretical uncertainties: the extraction of the top-quark pole mass has a theoretical uncertainty of around 300 MeV and cannot be determined with a precision better than  $\mathcal{O}(\Lambda_{QCD})$  [6]. In addition, incomplete knowledge of the hadronic final state leads to an uncertainty of a few hundreds MeV [5]. For the latter, one of the most significant uncertainties is related to the reconstruction of the  $W$  mass,  $M_W$ , after minimizing  $|M_{jj} - M_W|$ , where  $M_{jj}$  is the dijet invariant mass. The way how the large Breit-Wigner tails of the decay  $W \rightarrow 2 \text{ jets}$  is treated when the top quarks are reconstructed directly affects the reconstructed top mass [5]. A significant impact on the reconstructed top mass may come from non-perturbative phenomena, such as colour rearrangement [7] and Bose-Einstein effects [8], which are expected to shift the reconstructed masses in the  $W^+W^-$  and  $t\bar{t}$  production. Thus, any approach involving the reconstruction of  $W \rightarrow 2 \text{ jets}$  is bound to lead to a systematic shift for the top reconstruction. For example, it has been shown that the present implementation of the Bose-Einstein effect in a Monte Carlo model can contribute to a shift in the reconstructed top mass through a distortion of the  $M_{jj}$  spectrum [5]. Similar effects are expected for the color-reconnection phenomenon which is anticipated to be significant for the LC energies.

In this article, a simple reconstruction method which does not involve the direct measurement of the decay  $W \rightarrow 2 \text{ jets}$  is proposed. This method is a very general, and is suitable for the reconstruction of any process in which a particle ( $V$ ) and an anti-particle  $\bar{V}$  are produced and then decay as:

$$e^+e^- \longrightarrow V + \bar{V} \longrightarrow v_a V_a + v_b V_b$$

$$V_a \longrightarrow V_1 + \bar{V}_2, \quad V_b \longrightarrow V_3 + \bar{V}_4,$$

without *a priori* knowledge on the masses of the intermediate particles, denoted as  $V_a$  and  $V_b$ . The effectiveness of this method is based on the assumptions that the initial-state particles,  $V$  and  $\bar{V}$ , have similar (but not equal!) masses,  $|M_V - M_{\bar{V}}| \ll M_{V(\bar{V})}$ , and that the simplicity of  $e^+e^-$  annihilation allows to use the momentum conservation,  $\vec{P}_V + \vec{P}_{\bar{V}} = 0$ . These two requirements, together with the fact that both initial particles decay similarly into three other particles, are essential in the reconstruction of the invariant masses of  $V$  and  $\bar{V}$  through six jets in the final state.

## 2 Reconstruction procedure

We consider  $e^+e^-$  collisions in the laboratory frame. As a first step, six jets in the event have to be reconstructed. We use the  $k_\perp$  (Durham) algorithm [9], requiring exactly six

jets in every event, without any specific cuts on the transverse momenta and rapidity of the jets.

## 2.1 Event selection

To preselect hadronic events, we use the typical LEP cuts which take advantage of the energy-momentum conservation requirements:

$$\left| \frac{E_{vis}}{\sqrt{s}} - 1 \right| < \Delta_E, \quad \frac{|\sum \vec{p}_{||i}|}{\sum |\vec{p}_i|} < \Delta_{PL}, \quad \frac{|\sum \vec{p}_{Ti}|}{\sum |\vec{p}_i|} < \Delta_{PT}, \quad (1)$$

where  $E_{vis}$  is the visible energy,  $\vec{p}_{||i}$  ( $\vec{p}_{Ti}$ ) is the longitudinal (transverse) component of momentum of a final-state particle. The  $\Delta_E$ ,  $\Delta_{PL}$  and  $\Delta_{PT}$  are small adjustable parameters. The top events are characterized by a large amount of missing energy/momentum due to undetected neutrinos, therefore, the selection (1) is especially important as it helps to reject events with a significant fraction of neutrinos [5].

The jets in the all-hadronic top-decay channel should be well separated in the transverse momenta. The best way to do this is to apply a restriction on the values of  $y_6^{cut}$  used in the Durham algorithm to resolve six jets. We accept only events if  $y_6^{cut} > \Delta_y$ , with  $\Delta_y$  being a parameter to be found using a Monte Carlo simulation. A similar cut was applied for the JADE jet algorithm in the study of the all-hadronic top decay using the LCD Fast Simulation [3].

## 2.2 Top reconstruction

We start with the initial list of six jets with momenta  $p_i$ . These jets are merged into groups, with three jets in each group. Thus, every event can be considered to consist of pairs of the three-jet groups with momenta  $\{P_I(1), P_I(2)\}$ , where  $P_I(1) \equiv P_{i,j,m} = p_i + p_j + p_m$  is the four-momentum of each group, and  $P_I(2)$  was obtained analogously using the rest of the jets in the same event. In total, there are twenty three-jet groups, which can be arranged into ten three-jet pairs with non-identical momenta, i.e.  $I = 1, \dots, 10$ . Ideally, from these ten pairs of three-jet clusters, one should accept only one three-jet pair corresponding to two initially produced particles. In practice, it is difficult to find the correct assignments of jets due to fragmentation and detector effects. Therefore, a special selection should be performed in order to minimize the number of three-jet pairs. Assuming that the produced particles have similar masses, we accept such three-jet pairs if the invariant masses of the three-jet groups satisfy the condition  $|M_I(1) - M_I(2)| < \Delta_M$ , where  $M_I$  is the invariant mass of a three-jet group with the momentum  $P_I$ , and  $\Delta_M$  is a free parameter constraining the invariant masses of three jets inside each pair.

Next, energy-momentum conservation can be used to set an additional constraint on the momenta of three-jet groups within each three-jet pair. We accept only three-jet groups which are produced back-to-back, i.e. we require  $|\vec{P}_I(1) + \vec{P}_I(2)| < \Delta_P$ , where  $\Delta_P$  is again an adjustable parameter.

The following additional selection criteria may also be used:

- The list of three-jet groups contains top-quark candidates, which decay as  $t \rightarrow bW \rightarrow bq\bar{q}$ . In order to reduce the number of possible three-jet pairs, one can use an efficient double  $b$ -tagging, requiring one and only one  $b$ -initiated jet within each three-jet group. All three-jet pairs which have at least one three-jet group with two  $b$ -initiated jets have to be removed. This leads to six possible three-jet pairs, compared to ten if no  $b$ -tagging is used.
- Each three-jet group should contain two jets coming from the decay of the  $W$  boson. Thus, one can remove such three-jet groups which cannot be associated with the  $W$ -decay hypothesis. This can be done by accepting such three-jet pairs which have the invariant masses of any two jets inside the region  $|M_{jj} - M_W| < \Delta_W$ . This requirement is not advocated in this article as it makes the specific physics assumptions on the invariant mass and width of the  $W$  boson.

These two additional criteria are optional; in fact, we will show that even without them one can obtain a robust reconstruction procedure.

### 2.3 Monte Carlo studies

To illustrate the method outlined above, we first apply it to the all-hadronic top decays in  $e^+e^-$  annihilations at the centre-of-mass energy of  $\sqrt{s} = 500$  GeV generated using the PYTHIA 6.2 model [10]. The contribution from the initial-state radiation (ISR) can be rather significant at LC energies, thus this effect was included in the simulation. The mass and the Breit-Wigner width of the top quarks were set to the defaults values, 175 GeV and 1.39 GeV, respectively. The particles with the lifetime more than 3 cm are considered to be stable. Neutrinos were removed from the consideration.

In order to reconstruct the top quarks using the proposed method, one should define the following: a) the parameters for the event selection:  $\Delta_E, \Delta_{PL}, \Delta_{PT}, \Delta_y$ ; b) the parameters for the final reconstruction:  $\Delta_M$  and  $\Delta_P$ . The event-selection parameters should not be large in order to insure small contaminations from neutrinos resulting to a broad and asymmetric Breit-Wigner peak for the three-jet mass distribution. In this study, we will apply rather tight cuts:  $\Delta_E = \Delta_{PL} = \Delta_{PT} = 0.02$ . The parameter  $\Delta_y$  requires an additional study: Fig. 1 shows the distribution for the all-hadronic top decays and for  $e^+e^-$  inclusive events (but without the  $e^+e^- \rightarrow t\bar{t} \rightarrow 6 jets$  process) generated with the PYTHIA model. The top events are characterized by  $y_6^{cut} > \Delta_y = 2 \cdot 10^{-4}$ , thus this value is used for the studies below.

The parameter  $\Delta_M$  controls the maximum difference between masses of two top-quark candidates. It was set to 30 GeV, which is large enough to insure a reasonable event acceptance, but sufficiently small to exclude wrong assignments of jets. The parameter  $\Delta_P = 5$  GeV further reduces the contributions from unmeasured neutrinos. Note that the latter cut is not very important for the generator-level study, since the event selection is already very strong. In practice, such cuts should not be very tight to obtain a reasonable acceptance after a detector reconstruction.

Figure 2 shows the three-jet invariant masses after the selection procedure described above, but without the requirements of double  $b$ -tagging, and also without the cut on  $|M_{jj} - M_W|$ . Two different functions were used to fit the peak: a) the Breit-Wigner

distribution (with the fixed width of 1.39 GeV) convoluted with a Gaussian and b) the Breit-Wigner function alone. The first-order polynomial is used in order to describe the background in both cases. The motivation for the Gaussian convoluted with the Breit-Wigner function comes from the assumption that contributions of many independent effects (parton-shower splittings, hadronization and resonance decays) should yield a Gaussian-like distribution. As seen from Fig. 2, the best fit can be obtained by using the Breit-Wigner function alone, while the Gaussian does not describe adequately the tails of the mass distribution. Based on this empirical observation, we will use the Breit-Wigner function to fit the mass spectra before the LC detector simulation.

The fact that the Gaussian distribution fails to describe the mass spectrum might indicate a strong correlation between different effects leading to non-Gaussian broadening of the natural width. It was verified that a sum of two Gaussian distributions gives a better fit than the Gaussian distribution alone, but the Breit-Wigner still gives the best fit. It is likely that a sum of many Gaussian distributions should be used to fit the mass spectrum. In this case, an unknown weight for each Gaussian contribution would reflect the fraction of events with a particular property.

One interesting feature of the invariant-mass distribution shown in Fig. 2 is that it has no background in the region of small three-jet masses, where the major contribution from the QCD multi-jet background is expected. This can be explained as following: any misassignment of jets at a centre-of-mass energy far from the top-production threshold usually increases the observed three-jet invariant mass, since in this case the misassignment jet usually has a significant angle with respect to the rest of the jets in the three-jet group. This ultimately increases the three-jet invariant masses.

As was mentioned in the introduction, this method is expected to be less sensitive to the hadronic-final state uncertainties which usually arise when the invariant mass of the dijets from the decay  $W \rightarrow 2 \text{ jets}$  is reconstructed. Fig. 2 shows the three-jet invariant-mass distributions without and with the Bose-Einstein interference included. We use the so-called “BE32” type of the Bose-Einstein simulation, which is included in the PYTHIA 6.2 model [10]. It is clear that no any significant shift for the reconstructed top mass can be attributed to the Bose-Einstein effect when the proposed method is used for the top reconstruction.

### 3 Top reconstruction using the full detector simulation

The reconstruction of the top quarks after the full detector simulation was performed in a few steps:

1) Fully inclusive  $e^+e^-$  annihilation events were generated with the PYTHIA 6.2 model, which was based on the default parameters. Events with the  $W^+W^-Z$  and  $ZZZ$  production leading to six jets in the final state were not included in the simulation, as they have a small contribution ( $\sim 2\% - 4\%$ ). In total, 270k events were generated. This sample approximately corresponds to twenty days of the LC data taking.

2) From this sample,  $e^+e^- \rightarrow t\bar{t} \rightarrow \text{everything}$  events were passed through the full GEANT-based detector simulations. The number of such events was 9.6k. The

TESLA detector [11] simulation based on the BRAHMS 305 [12] program was used for the event reconstruction. Of particular importance for the present study are the tracking system based on the Time Projection Chamber (TPC) and the calorimeter (CAL). The TPC is surrounded by the CAL, which is longitudinally segmented into electromagnetic and hadronic sections. The electromagnetic calorimeter is based on tungsten absorber and silicon diode pads, while the hadronic part is an Fe/scintillating tile calorimeter. All particles in events were reconstructed using a combination of track and calorimeter information that optimizes the resolution of the reconstructed jets [13].

3) The rest of the sample (without the top quarks) was treated differently: Energies of the final-state particles in such events were smeared around the true values according to the Gaussian resolution functions in order to imitate the detector response. Charged hadrons (with energy denoted by  $E_{ch}$ ) were smeared using the Gaussian distribution with  $\sigma = 10^{-4}E_{ch}^2$ . Analogously, photon energies ( $E_\gamma$ ) were smeared using  $\sigma = 0.12\sqrt{E_\gamma}$ , while the energies ( $E_n$ ) of neutral hadron were distributed according to  $\sigma = 0.4\sqrt{E_n}$ . Particles close to the beam pipe were removed, to reproduce the geometrical acceptance of the LC detector.

The selection and the reconstruction of top quarks at  $\sqrt{s} = 500$  GeV are based on the parameters given in Table 1a). These parameters are the same for the generated and reconstructed event samples. For the former sample, neutrinos were removed, as well as particles which are inside the beam pipe. The cuts on the energy/momentum imbalance were determined after the study of the detector resolution, and were optimized to obtain a reasonable efficiency of the reconstruction. Figure 3 illustrates the distributions of the total event energy before and after the detector simulation. A significant missing energy due to neutrinos and the ISR is observed even before the event reconstruction. The event-selection cuts are by a factor two-three larger than the resolution on the corresponding variable. Events were removed if at least one lepton is found with an energy above 20 GeV; the motivation for this cut is clear from Fig. 4.

Figure 5 shows the three-jet invariant masses for the reconstructed all-hadronic decays in the process  $e^+e^- \rightarrow t\bar{t}$  before the detector simulation. The width of the Breit-Wigner distribution, 9.5 GeV, is somewhat larger than that shown in Fig. 2, since now a larger contribution from the missing energy/momentum is allowed to obtain a higher selection efficiency. This width will be used in the following figures for the Breit-Wigner function.

Figure 6 shows the three-jet invariant masses after the full detector simulation and event reconstruction. The background events from the non-top continuum were added after the Gaussian smearing. The cuts are the same as for Fig. 5, except for the cut on  $y_6^{cut}$ . A significant reduction of the background can be obtained by selecting events with  $y_6^{cut} > 2 \cdot 10^{-4}$ , as seen from Fig. 7. Note that this cut is the same as for the generator-level studies, since the LC detector simulation does not distort significantly the  $y_6^{cut}$  distribution.

Additional assumptions can further increase the signal-over-background ratio. For example, Fig. 8 shows that the cut on the invariant mass of two jets inside each three-jet group,  $|M_{jj} - M_W| < 15$  GeV, reduces the background. Further, a check using the generator-level reconstruction indicated that an efficient double  $b$ -tagging can decrease the background by  $\sim 50\%$ . This, however, has no a significant impact on the

Gaussian width, which is 5.0 – 5.5 GeV for the the current detector design and event reconstruction.

## 4 Top reconstruction at $\sqrt{s} = 800$ GeV

The proposed method is well suited for a higher centre-of-mass energy of  $e^+e^-$  collisions. The reconstruction is expected to be even more reliable: Since the hadronic jets are better collimated along the momenta of the produced top quarks, any wrong jet assignment significantly increases the invariant mass for such a miss-reconstructed top candidate. This should lead to a large invariant-mass difference between miss-reconstructed three-jet groups, therefore, such groups which will be removed by the cut on  $|M_I(1) - M_I(2)|$  more effectively.

At higher energies, however, missing event energy/momentum is larger due to higher energies of neutrinos. Therefore, the selection cuts should further be optimized to obtain a reasonable selection efficiency. Table 1b) shows the event-selection and top-reconstruction cuts applied for  $\sqrt{s} = 800$  GeV. We also use the same reconstruction cuts as for  $\sqrt{s} = 500$  GeV to be able to compare the results with the previous founding. Note that the  $y_6^{cut}$  distribution for  $\sqrt{s} = 800$  GeV is somewhat different than that shown in Fig. 1: now the distribution extends down to  $y_6^{cut} = 10^{-5}$ , and has a small peak at  $y_6^{cut} \sim 10^{-4}$ . This is due to a better collimation of jets originating from the top quark. It was found, however, that a decrease of  $\Delta_y$  for events at  $\sqrt{s} = 800$  GeV has a small impact on the final selection efficiency.

Figure 9 shows the three-jet invariant masses for  $e^+e^- \rightarrow t\bar{t}$  events generated with PYTHIA before the detector simulation. The PYTHIA event sample has the same size as for Sect. 3. The signal-over-background ratio is significantly larger for events at  $\sqrt{s} = 800$  GeV than for  $\sqrt{s} = 500$ , as expected.

Note that the efficiency of the top selection is less by a factor two than for  $e^+e^-$  annihilation at  $\sqrt{s} = 500$  GeV. It was found that most of the events were rejected by the cut  $|\vec{P}_I(1) + \vec{P}_I(2)| < \Delta_P$ , thus this cut is the main in reducing the fraction of events with significant missing energies from neutrinos. A check without the cut on the energy/momentum imbalance shows a very similar result as for the case without these cuts included. Generally speaking, the cuts on the event imbalance can be applied mainly to reduce the computational time before the top reconstruction, rather than to improve the signal-over-background ratio.

Figure 10 shows the reconstructed signal after the detector simulation and when events from the continuum were included. No any cuts on the dijet invariant mass were applied, i.e. this figure is equivalent to Fig. 7 for the lower centre-of-mass energy. The signal for  $\sqrt{s} = 800$  GeV has significantly less background, however, the number of the reconstructed top candidates is also smaller due rejection of events with large energy losses.

It is important to notice that the width of the Gaussian distribution is larger for  $\sqrt{s} = 800$  GeV than for  $\sqrt{s} = 500$  GeV. There are a few reasons for this. First, the energy resolution of the CAL is worse for higher jet energies. This, however, cannot completely explain the observed increase in the mass width. Again, let us remind that

jets from the decay of a single top are better collimated at  $\sqrt{s} = 800$  GeV, thus a larger degree of overlaps between energy deposits in the calorimeter is expected that makes more difficult to reconstruct the energy-flow objects. Furthermore, one should expect a stronger leakage for neural particles outside the calorimeter.

## 5 Snagging the top quarks using a neural network

Neural networks (NN) have seen an explosion of interest over the last years, and have been successfully applied for pattern recognition problems in particle physics. Based on the top-reconstruction approach described above, in this section we will devise a NN method to select top events using the hadronic-final-state signatures of the all-hadronic decays.

As a first step, one should define the variables for NN input which are likely to be influential. The event-shape variables represent the most efficient way to separate the  $t\bar{t}$  from the continuum [14, 4]. The thrust ( $T$ ) [15], major ( $Mj$ ) and oblateness ( $Ob$ ) event characteristics will be our primary choice. The allowed range for thrust is  $0.5 \leq T \leq 1$ , such that the isotropic events have  $T \sim 0.5$ , whilst a 2-jet configuration should have  $T \sim 1$ . We use as positive direction of the thrust axis the direction of the most energetic jet. The thrust axis is defined as the axis along which the projected energy flow is maximized. The major is sensitive to the energy flow in the plane perpendicular to the event thrust axis, and its direction is defined in the same fashion as thrust. The minor axis is the third axis, which is perpendicular to the thrust and major axis. The difference between the major and minor values is called the oblateness, such that  $Ob \sim 0$  corresponds to an event configuration symmetrical around the thrust axis. Figs. 11a)-c) show the values of the thrust, major and oblateness for the PYTHIA 6.2 model, after the energy smearing to imitate the LC detector response. The shaded band represents the  $e^+e^- \rightarrow t\bar{t} \rightarrow 6 jets$  events, scaled according to the predicted cross section. It is clear that the values of the thrust and the major have the best sensitivity to the top-quark production, while the oblateness reflects the properties of the top decays in less extent.

It is mandatory to use an additional information on the invariant mass of the decaying system, together with the variables discussed above which mainly focus on the topological properties of the event shapes. Since the top mass is approximately known, and because the production of two top quarks at  $\sqrt{s} \geq 500$  GeV is above the top-production energy threshold, an  $e^+e^- \rightarrow t\bar{t}$  event can be viewed as a simple two-body decay with non-overlapping decay products. The top events can be divided in two event hemispheres, each of which has an invariant mass close to the top mass. The hemispheres can be defined by using the thrust axis, such that particles with positive  $Z$  component belong to the first hemisphere, while particles with  $Z < 0$  form the second hemisphere. Fig. 11d) shows the invariant-mass distribution,  $M_2 = 0.5(M_a + M_b)$ , where  $M_a$  ( $M_b$ ) is the invariant mass of the hadronic system in the first (second) hemisphere. For the  $e^+e^- \rightarrow t\bar{t} \rightarrow 6 jets$  events, the invariant mass has a broad peak near the generated (true) top-mass value, while  $e^+e^-$  events without the all-hadronic top decays typically have rather low invariant masses.



Furthermore, since the all-hadronic top decay is characterized by a six-jet configuration, one can use this information for the top selection. Particularly,  $y_N^{cut}$  values of the resolution parameter of the Durham algorithm for which an  $N$ -jet configuration becomes an  $N + 1$  jet system can also be useful. We have already illustrated that the cut on  $y_6^{cut}$  alone has a significant impact on the selection of the all-hadronic top decays.

## 5.1 Standardizing inputs

The contribution of an input for a NN depends heavily on its variability relative to other inputs. Therefore, it is essential to rescale the inputs, so their variability reflects their importance. We will rescale some inputs to the interval  $[0, 1]$ , which is the most popular choice for the NN inputs.

In case of the event shape distributions, we do not use any rescaling, since all these variables are already in the interval  $[0, 1]$ . For the mass distribution  $M_2$ , we used the function  $A_1(\ln M_2 - A_2)$ , with  $A_1 = 3.4758$  and  $A_2 = 5.0106$ . This choice was advocated in [16], and here we only adjusted the free parameters  $A_1$  and  $A_2$ , such that this new variable is zero for  $m_t = 150$  GeV, and it equals to unity when  $m_t = 200$  GeV.

The situation with  $y_N^{cut}$  values is more complicated, since their values strongly depend on  $N$ . As example,  $y_2^{cut}$  for which 2 jets become a 3-jet system has a significantly larger value than  $y_{N>2}^{cut}$ . For the all-hadronic top decay, the relative importance of  $y_N^{cut}$  values for event configurations with large  $N$  is higher than for low  $N$ . Therefore, in order to treat all inputs on an equal footing, we transformed all  $y_N^{cut}$  values according to the expression  $Y_i = i^2 y_{i+1}^{cut}$   $i = 1 \dots 6$ , which increases the relative weights of  $y_N^{cut}$  values in the NN input for events with many jets.

## 5.2 Training sets

We have trained the NN to learn just one number in the range between 0 and 1. When the NN output is unity, this corresponds to the most probable top candidate in the all-hadronic decays.

A few data sets were used. The first event sample is for the NN training. It consists of 40k  $e^+e^-$  PYTHIA events with the ISR included. One half of this sample contains fully inclusive events but without the  $e^+e^- \rightarrow t\bar{t} \rightarrow 6 jets$  process, while another half contains the all hadronic decays of  $t\bar{t}$ . The top masses were generated according to the Breit-Wigner distribution with the nominal (peak) positions flatly distributed in the interval 150 – 200 GeV. The momenta of the final-state particles were smeared as discussed in Sect. 3. The second set contains also 40k events, half of them are the fully hadronic top decays. This set was used to assess the performance (generalization) of the learning, in order to avoid over-fitting.

## 5.3 Neural network architecture and the results

The neural network selection was based on the Stuttgart Neural Network Simulator [17] with the logistic activation function  $1/(1 + \exp(-x))$ . A feed-forward architecture with

one output node representing the probability of the observation of the fully hadronic top decays was used. For an input, we use nine nodes representing  $1 - T$ ,  $M_j$ , the rescaling value of the invariant mass,  $M_2$ , and six values of  $Y_i$  representing the Durham-algorithm resolution parameters. We investigated the effect of varying the number of hidden layers and nodes in these layers. It was found that one hidden layer with seven nodes was sufficient to achieve the best selection performance.

The neural net was applied to select the top events from the sample discussed in Sect. 3. Events were accepted if the NN output values are above 0.97. Figure 12 shows the NN output, which has a clear peak near unity.

Figure 13 illustrates the reconstructed top events after the NN event selection. The top reconstruction was the same as for Fig.6. The signal-over-background ratio is larger than that without the NN selection, as well as the statistical error on the top mass is smaller than for Fig.7-8. However, a small shift in the reconstructed mass was observed which should properly be taken into account after a correction procedure. In addition, the shape of the background is less understood than in case without the NN selection.

## 6 Accuracy on the top-quark measurements

The Monte Carlo luminosity used in this analysis corresponds to  $16 \text{ fb}^{-1}$  for  $\sqrt{s} = 500 \text{ GeV}$  and  $33 \text{ fb}^{-1}$  for  $\sqrt{s} = 800 \text{ GeV}$ . Our results indicate that the statistical error on the top-mass measurement for this luminosity is about  $380 - 450 \text{ MeV}$ . Thus, for an integrated luminosity of  $300 \text{ fb}^{-1}$ , corresponding to one to two years of running, the proposed method for the all-hadronic decay channel will lead to a statistical error of  $\delta m_t \sim 100 \text{ MeV}$  at  $\sqrt{s} = 500 \text{ GeV}$ . The statistical uncertainty on the mass measurement for  $\sqrt{s} = 800 \text{ GeV}$  is by a factor two larger due to a significant missing energy from neutrinos. Tables 2 and 3 show the results for  $\sqrt{s} = 500 \text{ GeV}$  and  $\sqrt{s} = 800 \text{ GeV}$ .

The direct measurement of the top-quark width in this decay mode is difficult. The reconstructed width is by more than a factor ten larger than the generated (true) top width. Therefore, other methods should be investigated to be able to measure the top width from the hadronic-final-state signatures of  $e^+e^-$  collisions.

One can also roughly estimate the statistical accuracy on the measurements of the total cross section for the all-hadronic top-decay channel. This study indicated that the number of the top candidates is around 2k for  $16 \text{ fb}^{-1}$ . This number of the top candidates was obtained from  $4224 \text{ } t\bar{t} \rightarrow 6 \text{ jets}$  events, thus the acceptance is  $\sim 24\%$ . For an integrated luminosity of  $300 \text{ fb}^{-1}$ , about 80k  $t\bar{t} \rightarrow 6 \text{ jets}$  events are expected assuming  $\sigma_{t\bar{t}} = 0.6 \text{ pb}$ . This leads to  $\sim 260 \pm 0.9 \text{ fb}$  for the observed cross section, thus the relative accuracy is 0.35%. After the event reconstruction,  $\sim 19200 \pm 124$  events are expected, leading to  $64.8 \pm 0.4 \text{ fb}$ , and to a relative accuracy of 0.6%.

## 7 Summary

For the first time, the all-hadronic top decays were studied using the full TESLA detector simulation, after taking into account a realistic contribution from multi-jet

QCD background. This was done using a new method of the reconstruction, which is expected to be less sensitive to experimental and theoretical uncertainties arising from the direct measurement of the dijets with the invariant masses close the  $W$  mass. Note that the method is a very general and can be used for the reconstruction of any two particles decaying into six jets in  $e^+e^-$  collisions. Also, the proposed approach is significantly simpler than the top-reconstruction method adopted at the TEVATRON, where a kinematic fit is used. The present method takes advantage of the fact that, in  $e^+e^-$  annihilation, the entire hadronic event can be reconstructed. Therefore, essentially all produced particles can be grouped into jets using an exclusive jet algorithm, while energy-momentum conservation provides an additional handle for the top reconstruction. In contrast, the reconstruction of top quarks at the TEVATRON and LHC is characterized by a large missing energy along the beam directions, and by the use of inclusive jet algorithms which combine only a relatively small fraction of the produced hadrons into jets. We did not use the double  $b$ -tagging to obtain the top signal; we have verified that the  $b$ -tagging reduces the QCD background, but does not have a significant impact on the reconstructed width of the top quark.

The TESLA detector resolution for the top-mass measurement based on the energy-flow algorithm is  $5 - 5.5$  GeV for  $\sqrt{s} = 500$  GeV. This value is almost independent of method used to reconstruct the top quarks. For  $\sqrt{s} = 800$  GeV, the detector resolution is 9.5 GeV. Such an increase is due to higher jet energies, larger overlaps between energy deposits used for the energy-flow objects, as well as a larger calorimeter leakage. These two numbers can be used for comparisons with other detector designs and/or other methods of the event reconstruction. Note that even before the detector simulation, a significant width for the three-jet mass spectrum due to fragmentation effects is observed, thus the reconstruction of the top width from hadronic jets is very unlikely.

In this paper, we have estimated the typical statistical uncertainties on the top mass measurement, as well as the statistical uncertainty anticipated for the top-quark production cross section in the all-hadronic decay channel. The method leads to a statistical uncertainty of  $\delta m_t \simeq 100$  MeV for the modest value of the luminosity,  $300 \text{ fb}^{-1}$ . This uncertainty is compatible with the statistical precision for the most promising lepton-plus-jets decay channel at the LHC [2], and is well below the theoretical systematic uncertainty anticipated for the pole top mass. An essential aspect of this method is to understand limitations arising from experimental systematic uncertainties. However, this study has not been carried out yet.

## References

- [1] K. Tollefson and E.W. Varnes, *Annu. Rev. Nucl.* **49**, 435 (1999).
- [2] *Top quark physics*, ed. M. Beneke et al. Proceedings of the workshop "1999 CERN Workshop on SM physics at the LHC", hep-ph/0003033, 1999.
- [3] M. Iwasaki. Presented at the world-wide study of physics and detectors for future linear colliders (LCWS99), (Sitges, Barcelona, Spain, 1999) OREXP 99-04, hep-ex/9910065 (1999).
- [4] S. Moretti, *Eur. Phys. J.* **C 9**, 229 (1999);  
S. Moretti, *Nucl. Phys.* **B 544**, 289 (1999);  
F. Gangemi et al., *Nucl. Phys.* **B 559**, 3 (1999).
- [5] S.V. Chekanov, *Eur. Phys. J.* **C 26**, 173 (2002).
- [6] M. Beneke, *Phys. Lett.* **B 434**, 115 (1998);  
A.H. Hoang et al., *Phys. Rev.* **D 59**, 114014 (1999);  
A.H. Hoang et al., *EPJdirect* **C 3**, 1 (2000).
- [7] T. Sjöstrand and V.A. Khoze, *Z. Phys.* **C 62**, 281 (1994);  
V.A. Khoze and T. Sjöstrand, *Eur. Phys. J.* **C 6**, 271 (1999);  
A. Ballestrero et al., *Z. Phys.* **C 72**, 71 (1996);  
V.A. Khoze and T. Sjöstrand, *Eur. Phys. J. direct* **C 2**, 1 (2000);  
V.A. Khoze and T. Sjöstrand, *QCD Interconnection Studies at Linear Collider*, in *Physics and Experimentation at a Linear Electron-Positron Collider, Vol.1*, ed. T. Behnke et al., p. 257. DESY-01-123F, 2001.
- [8] L. Lönnblad and T. Sjöstrand, *Phys. Lett.* **B 351**, 293 (1995);  
S.V. Chekanov, E.A. De Wolf, W. Kittel, *Eur. Phys. J.* **C 6**, 403 (1999).
- [9] S. Catani et al., *Phys. Lett.* **B 269**, 432 (1991).
- [10] T. Sjöstrand et al., *Comp. Phys. Comm.* **135**, 238 (2001).
- [11] *Technical Design Report, Part IV, "A Detector for TESLA"*, ed. T. Behnke et al. DESY-2001-011, 2001.
- [12] T. Behnke et al., *BRAHMS: A Monte Carlo for a Detector at 500/800 GeV Linear Collider*, in *Physics and Experimentation at a Linear Electron-Positron Collider*, ed. T. Behnke et al., p. 1425. DESY-01-123F, [http://www-zeuthen.desy.de/lc\\_repository/detector\\_simulation/dev/BRAHMS/](http://www-zeuthen.desy.de/lc_repository/detector_simulation/dev/BRAHMS/), 2001.
- [13] V.L. Morgunov, *Energy-flow Method for Multi-jet Effective mass Reconstruction in the Highly Granulated TESLA Calorimeter*. APS/DPF/DPB Summer Study on the Future of Particle Physics (Snowmass 2001), <http://www.slac.stanford.edu/econf/C010630/proceedings.shtml>, 2001.

- [14] P. Igo-Kimens and J. H. Kühn, *Proc. of the Workshop on "e<sup>+</sup>e<sup>-</sup> Collisions at 500 gev. The Physics Potential"*. (Munich-Annecy-Hamburg) DESY 92-123, 1992.
- [15] S. Brandt et al., *Phys. Lett.* **12**, 54 (1964);  
E. Fahri, *Phys. Rev. Lett.* **39**, 1587 (1977).
- [16] L. Lönnblad, C. Peterson and T.Rögva, *Phys. Lett.* **B 278**, 181 (1992).
- [17] A. Zell et al., *Stuttgart Neural Network Simulator (SNNS), Version 4.2*. Unpublished.

	$\Delta_E$	$\Delta_{PL}$	$\Delta_{PT}$	$\Delta_y$	$\Delta_M$ (GeV)	$\Delta_P$ (GeV)
a) PYTHIA, $\sqrt{s} = 500$ GeV	0.07	0.04	0.04	$2 \cdot 10^{-4}$	40	20
b) PYTHIA, $\sqrt{s} = 800$ GeV	0.4	-	0.3	$2 \cdot 10^{-4}$	40	20

Table 1: The parameters used for the selection and reconstruction of the top quarks in  $e^+e^-$  annihilation at: a)  $\sqrt{s} = 500$  GeV; b)  $\sqrt{s} = 800$  GeV.

PYTHIA, $\sqrt{s} = 500$ GeV	$\delta m_t$ (GeV)	BRW width (GeV)	Gaussian width (GeV)
Generated	0.030	$9.5 \pm 0.4$	-
a) Reconstructed	0.105	9.5 (fixed)	$5.0 \pm 0.2$
b) Reconstructed (NN)	0.087	9.5 (fixed)	$5.2 \pm 0.1$

Table 2: The statistical uncertainties on the top-mass measurement assuming an integrated luminosity of  $300 \text{ fb}^{-1}$  for  $e^+e^-$  annihilation events at  $\sqrt{s} = 500$  GeV. The table also shows the typical reconstructed widths for the cases: a) without using the NN (see Fig. 7) and b) with the NN selection (see Fig. 13).

PYTHIA, $\sqrt{s} = 800$ GeV	$\delta m_t$ (GeV)	BRW width (GeV)	Gaussian width (GeV)
Generator level	0.04	$7.7 \pm 0.4$	-
Reconstructed level	0.230	7.7 (fixed)	$9.5 \pm 0.4$

Table 3: The statistical uncertainties on the top-mass measurement for  $e^+e^-$  annihilation events at  $\sqrt{s} = 800$  GeV assuming an integrated luminosity of  $300 \text{ fb}^{-1}$ . The table also shows the typical reconstructed widths.

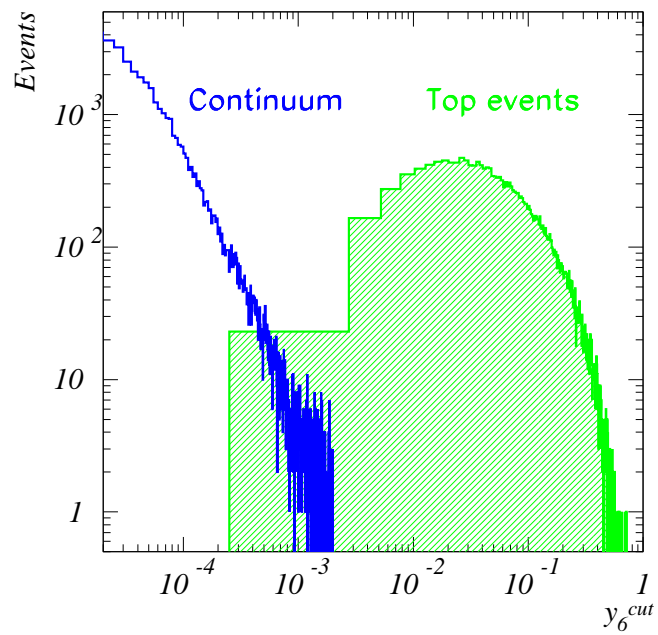


Figure 1: The values of  $y_6^{cut}$  for the all-hadronic top decays and for the rest of inclusive  $e^+e^-$  sample (continuum) generated with the PYTHIA model.

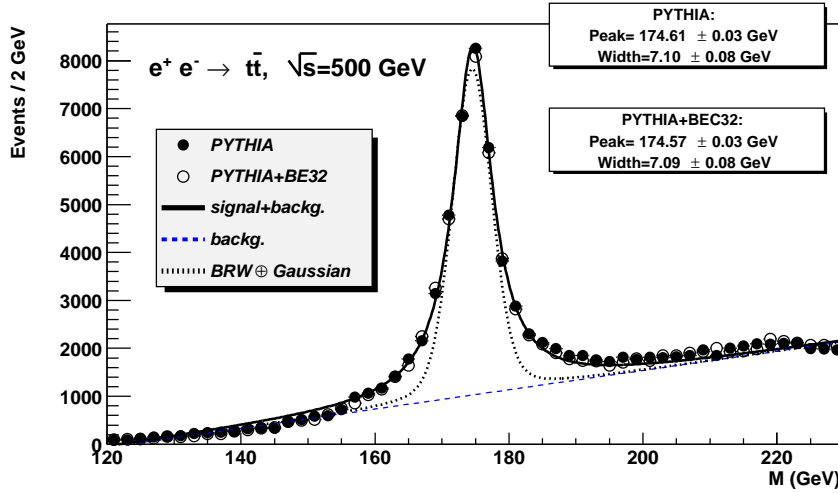


Figure 2: The distribution of three-jet invariant masses for  $e^+e^- \rightarrow t\bar{t} \rightarrow 6jets$  events at  $\sqrt{s} = 500$  GeV. The all-hadronic decay channel was generated with the PYTHIA model with (open dots) and without (solid dots) the Bose-Einstein effect. The peak position and the width were determined from the Breit-Wigner distribution, which gives the best  $\chi^2$  for the fit. A Gaussian convoluted with the Breit-Wigner distribution (with the fixed width of 1.39 GeV) is also shown (dashed line). The first-order polynomial is used to describe the background. The solid line shows the fit for the invariant mass obtained from the PYTHIA models without the BEC32 effect included.

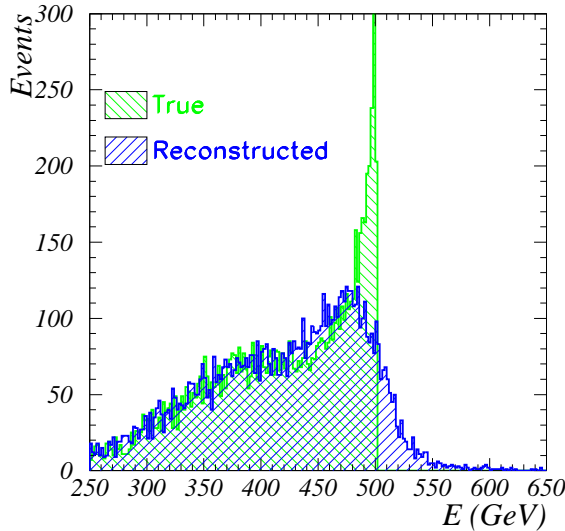


Figure 3: The distributions of the total event energies of  $e^+e^- \rightarrow t\bar{t}$  events before and after the LC detector reconstruction.



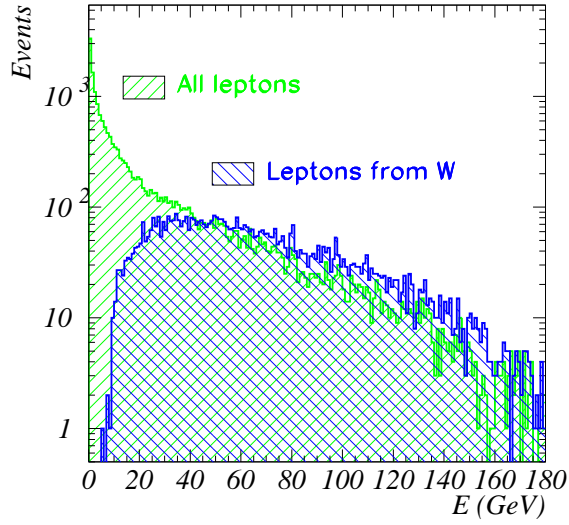


Figure 4: The reconstructed energies of the final-state leptons for semileptonic top decays and for the  $e^+e^- \rightarrow \text{everything}$  events.

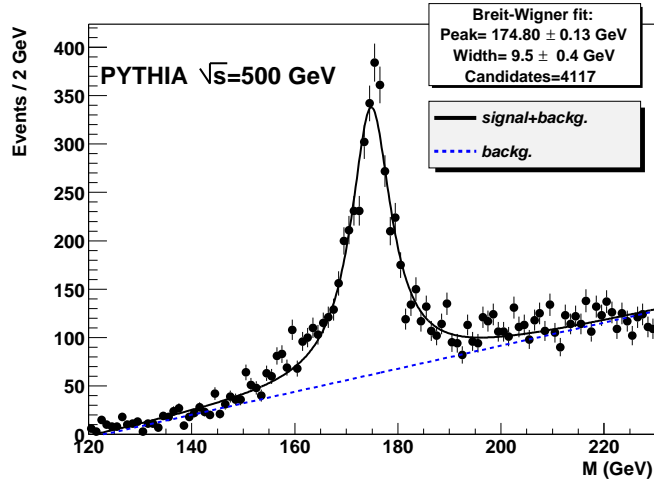


Figure 5: The invariant-mass distributions for three-jet clusters for  $e^+e^- \rightarrow t\bar{t}$  process at  $\sqrt{s} = 500$  GeV generated using the PYTHIA model before the LC detector simulation. The all-hadronic decays were selected and reconstructed using the parameters given in Table 1a).

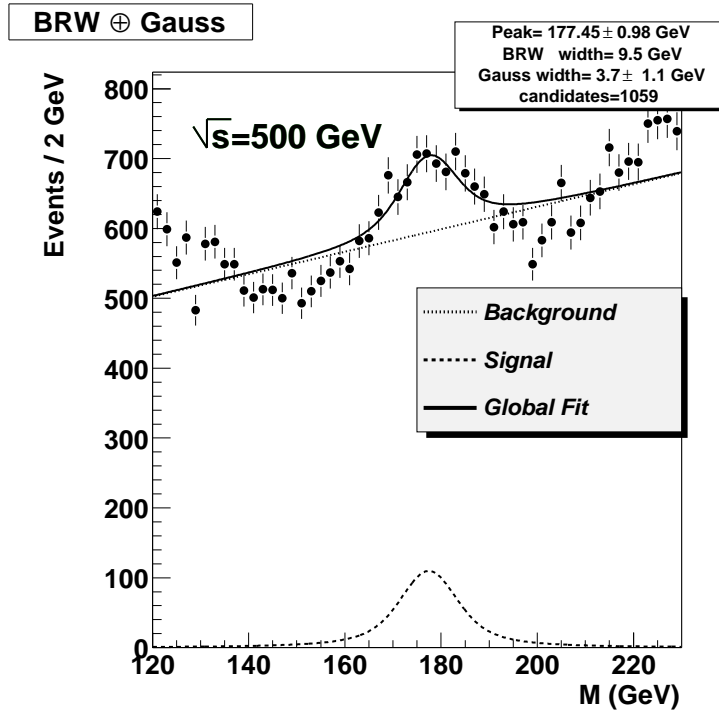


Figure 6: The invariant-mass distributions for three-jet pairs obtained from the fully inclusive  $e^+e^-$  PYTHIA events. Events  $e^+e^- \rightarrow t\bar{t}$  were passed through the full detector simulation, while the continuum was obtained after the Gaussian smearing of the original particle momenta. The top events were selected and reconstructed using the parameters given in Table 1a), but without the cut on  $y_6^{cut}$ . The fit is based on the Breit-Wigner function convoluted with a Gaussian, plus a linear function to describe the background. The width of the Breit-Wigner distribution is fixed to 9.5 GeV (see Fig. 5).

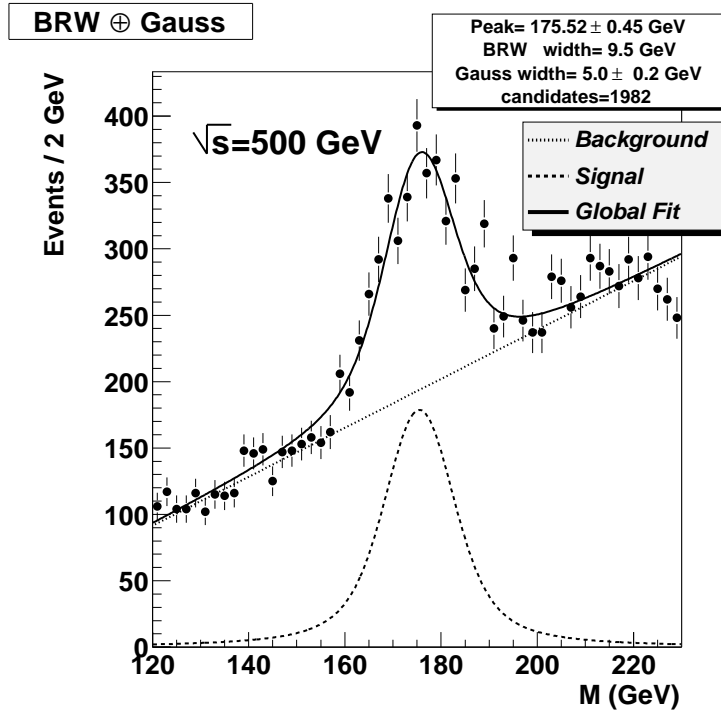


Figure 7: Same as Fig. 6, but after applying the cut  $y_6^{cut} > 2 \cdot 10^{-4}$ .

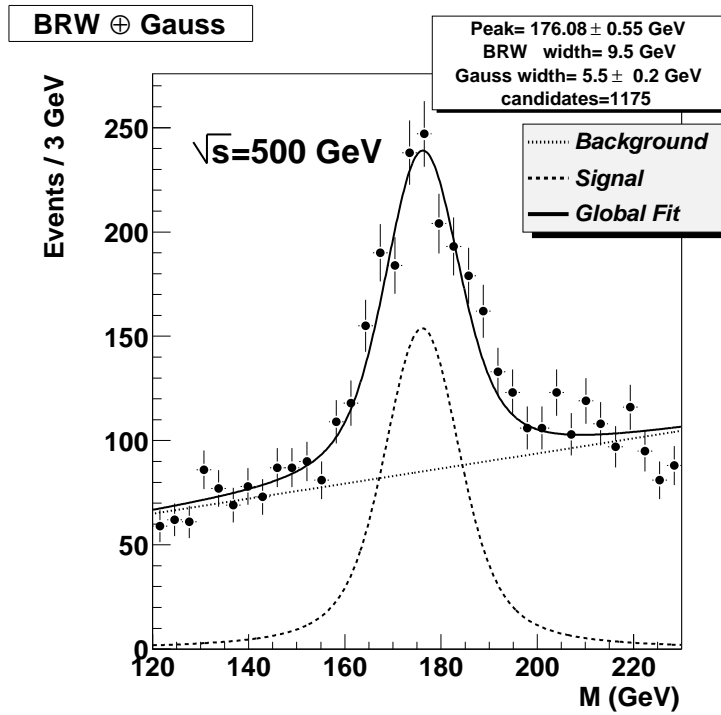


Figure 8: Same as Fig. 7, but in addition, only three-jet groups are shown which have at least one jet pair with  $|M_{jj} - M_W| < 15$  GeV.

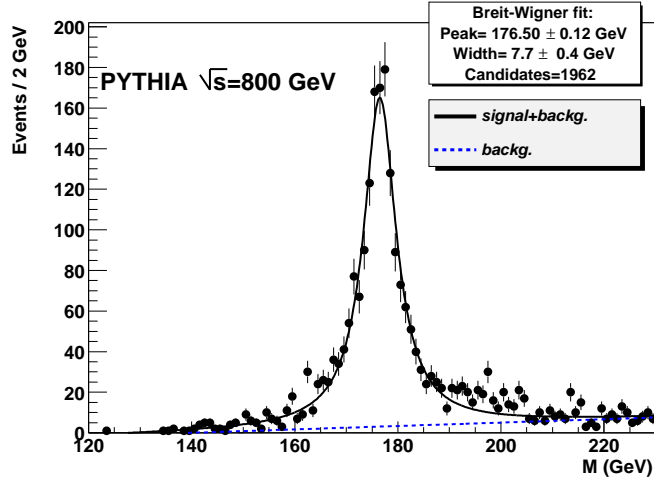


Figure 9: The invariant-mass distributions for three-jet clusters for  $e^+e^- \rightarrow t\bar{t}$  process at  $\sqrt{s} = 800$  GeV generated using the PYTHIA model. The all-hadronic decays were selected and reconstructed using the parameters given in Table 1b).

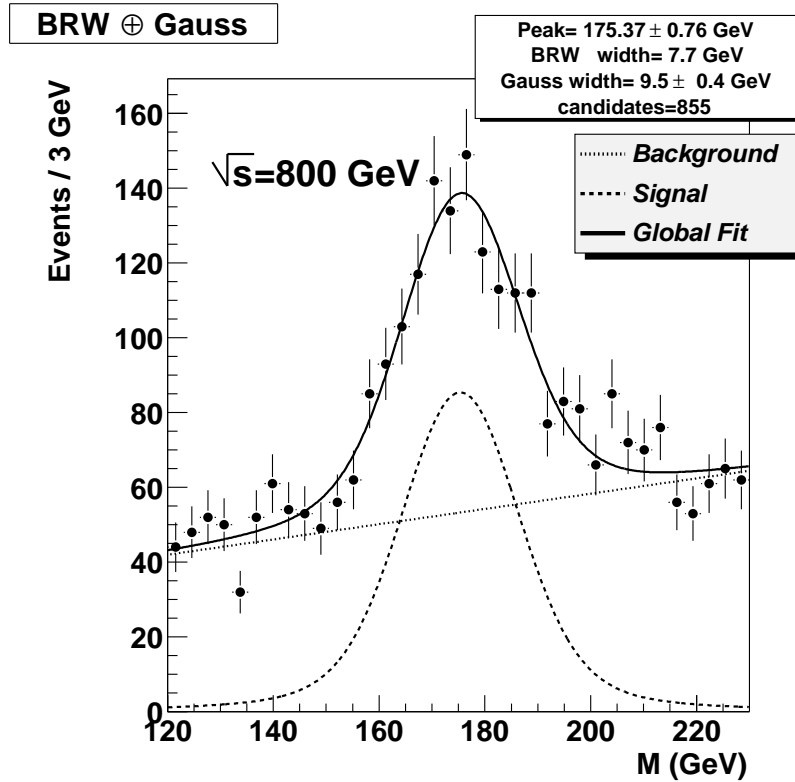


Figure 10: The reconstructed invariant masses for the all-hadronic top-decay channel generated with PYTHIA for  $\sqrt{s} = 800$  GeV after the LC detector simulation. The applied cuts as for Fig. 7. The Breit-Wigner width is taken from Fig. cap:tru2.

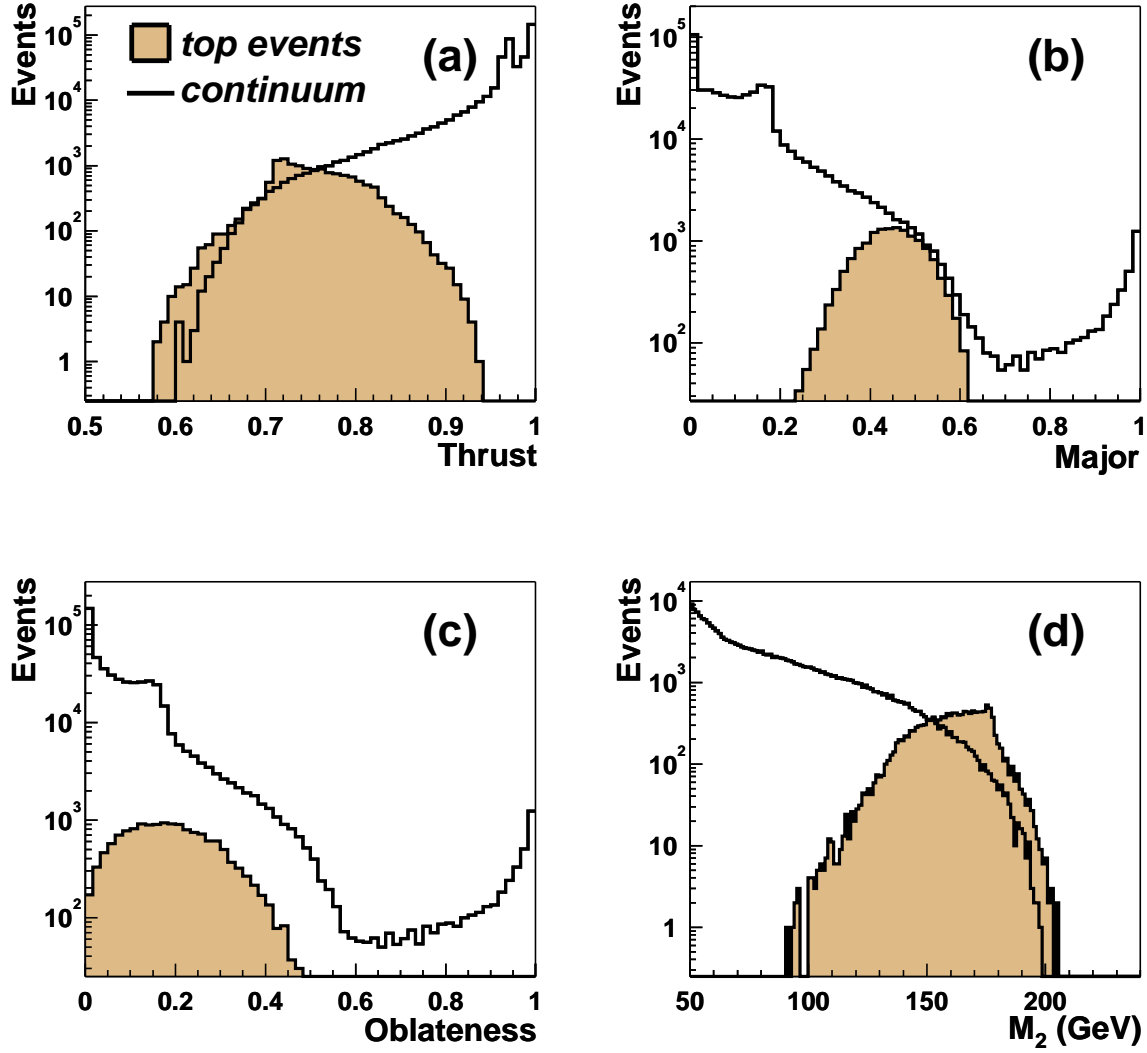


Figure 11: The values of the thrust, major, oblateness and the invariant masses of event hemispheres for fully inclusive  $e^+e^-$  PYTHIA events generated without the  $t\bar{t} \rightarrow 6jets$  process and for the all-hadronic top decays (shaded area).

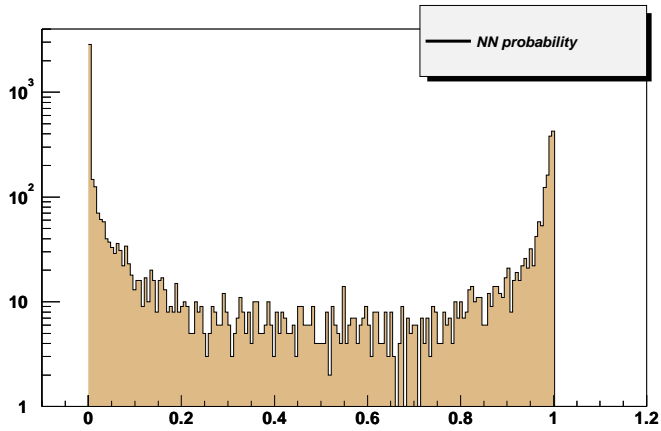


Figure 12: The output of the neural network for the fully inclusive PYTHIA events after the Gaussian smearing of particle momenta to imitate the LC detector response.

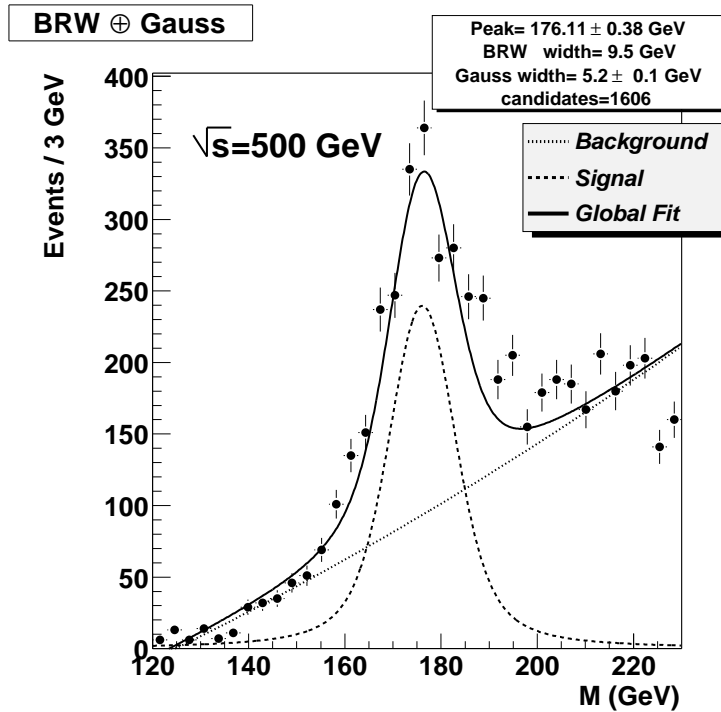


Figure 13: The invariant-mass distribution for three-jet clusters after the NN selection. The event selection as for Fig. 6.